OCEAN APPLICATIONS TECHNICAL NOTE 23.

HadCM3 Sensitivity Tests with Tuned Eddy Parametrization Schemes

by

Peili Wu and Chris Gordon.

Met Office
FitzRoy Road, Exeter, Devon. EX1 3PB

HadCM3 Sensitivity Tests with Tuned Eddy Parameterization Schemes

by

Peili Wu and Chris Gordon

Ocean Applications Branch, Meteorological Office

Abstract

Eddy parameterisation schemes play an important part in climate models for heat and salt transports. A refined scheme of the GM (Gent and McWilliams 1990) parameterisation proposed by Visbeck *et al.*(1997) has been used in the ocean part of HadCM3 control integration, but there are parameters in the scheme that need to be tuned for a particular model configuration.

This note reports several sensitivity experiments with HadCM3 on the GM scheme. It shows that the model is less sensitive to the eddy transfer coefficient than to the background values used in the model where the calculated GM coefficient falls below that threshold. We also show by comparison how variations of the GM scheme can affect the model errors, particularly in the North Atlantic Ocean. It is indicated that excessive GM transport could be partly responsible for the warm/salt anomalies in the North Atlantic seen in the HadCM3 control integration.

1 Introduction

HadCM3 is acknowledged to be one of the best climate models in the world at the present time. It has been successfully run for over 1000 years without serious drift in sea surface temperature (SST) and sea-ice extents under no flux corrections. It simulates realistic climatic states as well as natural variabilities for both the atmosphere and the oceans (see Gordon *et al.* 1999 for a detailed description of the model). Despite these successes, there are still problems that need to be addressed. One is a drift of water mass properties in the deep oceans. Although the global mean temperature and salinity drifts are small, they are significant in some individual basins. For example, in the North Atlantic, the long term mean temperature at intermediate depths can be more than 3°C warmer and salinity more than 0.5psu higher than the Levitus climatology. As shown in Fig.3 of Gordon *et al.*(1999), there is a trend of warming/freshening in the upper 1000m of the ocean but cooling/salinifying in the deep oceans in a global average. The accumulated effect of this trend translates into increased vertical stratification and hence effectively stabilises the global ocean in an average sense, which makes it harder for convection and overturning to take place. As shown in Fig.1, a large volume of over-dense water has been added to the deep layers below 2000m, where the average potential density (σ_θ) has increased from 27.8 to 27.9, over a period of 500 years. Preliminary study has shown that a large part of these errors originates from the intermediate depths of the model's North Atlantic Ocean which also contributes a big share to the global mean. Waters advected into the region of the North Atlantic subpolar gyre, the Greenland Sea, the Norwegian Sea and the Labrador Sea at intermediate depth are much too warm and salty. This bias of water mass properties at intermediate depth is then passed onto the North Atlantic deep water by convection and mixing of straits outflows.

The original motivation of this work was to investigate the long term drift of water mass properties in the model in order to improve their representation in future versions of the model. To identify exactly what causes the model to drift in such a way is not straight forward when the model's physics and numerics have reached such a complexity as in HadCM3. One potential approach would be to carry out a tendency analysis to itemise individual contributions to the total rate of change, similar to the "initial tendency error" method which Klinker and Sardesmukh (1992) and Milton (1994) used with atmospheric models. An analysis of the evolution of the systematic errors in the coupled model has shown that the subsurface error patterns after many centuries can also be found, with reduced amplitude, in short 10 year coupled runs. In these short simulations the ocean is closer to climatological initial conditions and the source of the model drift is therefore easier to identify. A term balance was carried out to identify the major contributors to the drifts. One of the most important arose from the eddy parameterization, the GM scheme (Gent and McWilliams 1990).

The GM scheme has now become an important part of z-coordinate coarse resolution climate models. It has clear advantages over horizontal mixing in parameterizing the effect of unresolved meso-scale eddies, and has proven to greatly improve model performance (e.g. Hirst and McDougal, 1996). The inclusion of the GM scheme in the Hadley Centre climate model has led to significant improvements, for example in the simulation of the meridional overturning and the North Atlantic current (Wright, 1997). How to choose the mixing coefficient is still ongoing research. Bryan *et al.*(1999) have recently compared several proposed formulations with eddy permitting model simulations and concluded that the scheme proposed by Visbeck *et al.*(1997), which is also implemented in HadCM3 (see Wright, 1997), provides the best fit. However, the Visbeck scheme contains parameters that need to be verified and tested. Sensitivity tests on these are desirable and useful for future improvement of model performance, in particular to find out if and to what degree the GM scheme is responsible for the detected model errors in the HadCM3 control run.

2 Eddy Parameterization

Some form of diffusion parameterization is always required to represent sub-grid scale processes in coarse resolution models. Apart from turbulent mixing and diffusion, the unresolved meso-scale eddies (analogous to synoptic disturbances in the atmosphere) in the ocean part of climate models deserve particular attention for their role in the transport of heat and other tracers in the ocean. The GM scheme is designed to parameterize this process in an adiabatic form of thickness diffusion of isopycnal layers or inverse density gradient, which mimics the physical process of baroclinic instability to release the available potential energy. It is the adiabatic form that makes the scheme physically much more realistic compared to the traditionally used horizontal mixing scheme, because it better conserves water mass properties when removing instabilities as observations have suggested. Therefore, the scheme should give a better simulation of the thermohaline circulation at climate time scales.

The GM scheme can be implemented by adding an "eddy induced transport velocity" (Gent *et al.* 1995) to the tracer equations in the form of

$$\boldsymbol{u}^* = -(K\frac{\nabla_h \rho}{\rho_z})_z, \qquad w^* = \nabla_h \cdot (K\frac{\nabla_h \rho}{\rho_z})$$

and

$$(\boldsymbol{u}^* + w^*\boldsymbol{k}) \cdot \boldsymbol{n} = 0$$

where $-\nabla_h \rho / \rho_z$ is the slope of the isopycnal surface, ρ the density, K the thickness diffusion coefficient, $\boldsymbol{k}$ the unit vertical vector and $\boldsymbol{n}$ the unit vector normal to the boundaries. Tracers are then advected by the "effective transport velocity" $(\boldsymbol{U}, W)$ rather than the large scale velocity $(\boldsymbol{u}, w)$ alone, where

$$\boldsymbol{U} = \boldsymbol{u} + \boldsymbol{u}^*, \qquad W = w + w^*.$$

The simplest form of the GM scheme is to assume a constant mixing coefficient K such as in Danabasoglou and McWilliams (1995), Hirst and McDougall (1996). Held and Larichev (1996) suggest that a spatially variable mixing coefficient will be more appropriate. This is based on the fact that eddy field in the ocean is spatially inhomogeneous with increased meso-scale variability generally found in the vicinity of strong lateral density gradients. Visbeck *et al.*(1997) have further explored this aspect based on the earlier ideas of Green (1970) and Stone (1972) about eddy transfer properties in the atmosphere. The eddy mixing coefficient K can be linked to the Eady growth rate of baroclinically unstable waves $(f/\sqrt{Ri})$ and the width of the baroclinic zone (l) such that

$$K = \alpha \frac{f}{\sqrt{Ri}} l^2,$$

where f is the Coriolis parameter and α is an unknown called the constant of proportionality (Visbeck *et al.*, 1997) or the efficiency constant (Spall and Chapman, 1998). The Richardson number Ri is defined as $Ri = (N/U_z)^2$, where N is the buoyancy frequency, $N^2 = \frac{g}{\rho_0}\frac{\partial \rho}{\partial z}$ whereas g is the acceleration due to gravity and ρ_0 a reference density. The mixing coefficient K can then vary both spatially and temporally when α is given. How to choose the value of α is still uncertain. Visbeck *et al.*(1997) recommended $\alpha = 0.015 \pm 0.005$ from their comparisons of parameterized and resolved parallel experiments with three oceanic scenarios. The resulting K can range from 300 for a convective chimney to $2000m^2/s$ for a wind-driven channel. The real "universal" value of α (if there is one) remains to be defined, although all the suggested values are not "far" from each other. The smallest is the one suggested by Green (1970) of 0.005, and the largest 0.045 came from a recent paper by Spall and Chapman (1998). It is of interest and importance to investigate how sensitive climate models are to changes of α. Do we need to limit K to a certain range and where should the boundaries be set?

3 The Experiments

Four experiments have been carried out each for 10 years. The mixing coefficient of the GM scheme K is variable in both time and space following Visbeck *et al.*(1997). However, boundaries are artificially set to limit K to stay within the range of $[K_{min}, K_{max}]$. This is primarily to prevent potential numerical problems. Model sensitivity to both K_{min} and K_{max} as well as the eddy transfer coefficient α needs to be tested. An extra option for using the GM scheme as a biharmonic diffusion with a constant coefficient K_b put forward by Roberts and Marshall (1998) has also been made available in the coupled model. It is possible to completely switch off the Visbeck scheme while the biharmonic GM diffusion is active. So there are 4 tunable parameters in our experiments, K_{min}, K_{max}, α and K_b. Table 1 compares the different parameters used for each experiment. Other model parameters are the same for all the experiments. The time mean of the entire 10 model years of each experiment are used to compare error differences for water mass properties. All experiments are initialised with Levitus climatology and the errors are referred to the deviations of model climatology from it.

The implementation of the Visbeck *et al.*(1997) scheme in the Hadley Centre climate model has been reported by Wright (1997). The Richardson number required for the calculation of thickness diffusion coefficient K is replaced by a vertical average $\overline{Ri}$ over the upper 2000m, following Treguier *et al.*(1997). The width of the baroclinic zone (l) is then defined by the spatial scale at which the local Eady growth rate or the

TABLE 1. List of the Experiments

Experiment	$K_{min}(m^2/s)$	$K_{max}(m^2/s)$	α	$K_b(10^{11}m^4/s)$
ABRJC	350	2000	0.015	0
ABRJD	100	2000	0.0075	0
ABRJF	100	2000	0.045	0
ABRJI	10	2200	0.005	3.9149

inverse time scale $(f/\sqrt{Ri})$ exceeds $1.4 \times 10^{-6}s^{-1}$, a number that was determined by experiment. The values of K are then calculated in the model daily within a range set by $[K_{min}, K_{max}]$. The first experiment ABRJC is a re-run of the HadCM3 control experiment (AAYFA) but with the version 4.5 of HadCM3. We refer to it as our control run. The major differences between the two model versions are the correction of a minor error in the Visbeck scheme (mainly affecting the region of the ACC) and the inclusion of a new tapering scheme to smooth the vertical transition from the mixed layer to the main thermocline when calculating the value of K. This may have some effects on the GM transports in the upper thermocline.

4 The Results

We will first compare the 4 experiments globally with zonal averages of water properties and then specifically concentrate on the North Atlantic. We use the 10 year mean fields to limit the impact of interannual variability. Since the deep ocean is too slow to respond in 10 years, only the upper 1000m is plotted. Because the eddy parameterization scheme is mainly acting in the main thermocline, one should focus on the difference below the mixed layer when comparing the experiments. Therefore, the top 100m is also excluded from the plots. The actual differences between the experiments are very small for the excluded parts, as expected. Before we start to compare the experiments, we must bear in mind that we are testing a fully coupled global ocean-atmosphere model and the total "model errors" may come from many different factors including numerical schemes and physical parameterizations. Our focus is on the differences that have been brought about by the changes of model parameters.

Figure 2 shows the global zonal mean errors of temperature and salinity averaged over the 10 model years for the control run, ABRJC. Model errors appears mainly in three regions: the Southern Ocean around the ACC, the northern upper subtropical ocean and the northern mid-high latitudes with extended depth. The Southern Ocean errors are small compared to the northern oceans. The northern mid-high latitudes have the most serious model errors, not only because of their amplitude and depth but also because of their direct link with the deep water and model drift in the North Atlantic as we shall see later. The error patterns for the 4 experiments remain similar but the amplitudes vary as we change the strength of the eddy parameterization. The major differences between the experiments appear only in the northern hemisphere between 50 to 70°N for temperature and 30 to 70°N for salinity. Therefore, we show the whole domain only for the control run, focusing on the latitudes where major differences exist when comparing the 4 experiments (see Figs.3 and 4).

Now let us compare the differences between the experiments. In Fig.3, the shaded areas are where the errors exceed $2°C$ and the contour intervals are $0.5°C$ between two solid or dashed contours but $0.25°C$ from a solid to the next dashed contour. In Fig.4, the shaded areas indicate where salinity errors are greater than 0.1psu. The contour intervals are 0.05psu between two solid or dashed lines but 0.025psu from a solid to the next dashed contour. Comparing the 4 experiments in Fig.3, we find similar error patterns but the amplitudes differ mainly between the control run and the other 3 with ABRJI showing the least errors. There are two maxima of errors in the plots; from ABRJC to ABRJI the maximum in the shaded area is reduced from above $2.75°C$ to below $2.25°C$ and the $0.75°C$ in the south disappears from ABRJI. The size of the shaded area is also reduced. The error patterns of temperature and salinity are closely correlated. Figure 4 presents a similar story, although salinity errors seem to be spread more widely with the southern error maxima located further south than temperature between 40 and $45°N$. The tendency of error reduction through the experiments for temperature is also true for salinity. From ABRJC to ABRJI, the reduction of salinity errors in the northern maximum around $65°N$ is more than 0.1psu, and the shaded area in the south is almost eliminated from ABRJI.

Figures 5 and 6 are the same as figures 3 and 4 but for the North Atlantic ocean only. In Fig.5, the shaded area marks temperature errors exceeding $2°C$, and in Fig.6

the shaded area is where the salinity errors are greater than 0.2psu. As mentioned previously, the North Atlantic contributes most of the water mass errors to the global zonal mean at the intermediate depth. A reduction of the model drift here is also important for the long term model integration, because these errors in water mass properties will be carried down to the bottom by the deep convection and propagate along the global conveyer belt. As we can see by comparison with figures 3 and 4, the errors in the North Atlantic are larger than the global mean errors. The comparison between the 4 experiments in the North Atlantic confirms what has been described above. Both temperature and salinity (figures 5 and 6) show a significant error reduction in ABRJI over the control run. In temperature the amount of error reduction in the shaded area is about $1°C$. The reduction of salinity errors is even clearer. From ABRJC to ABRJI, the maximum salinity error near $65°N$ is reduced from above 0.175psu to just above 0.1psu. The shaded area near $45°N$ disappears in ABRJI and the maximum value is reduced from above 0.3psu to below 0.2psu.

A comparison between ABRJC and the HadCM3 control run (AAYFA) has shown that the new version of the model does not lead to a significant reduction in model errors, although differences exist. However, the 3 experiments with reduced K_{min}, namely ABRJD, ABRJF and ABRJI, generally show smaller errors compared to ABRJC. The difference between ABRJD and ABRJF, which have the same K_{min} but considerably different α, is however very small. This seems to suggest that the model is more sensitive to the change of K_{min}, or the value of K_{min} used in the HadCM3 control experiment was probably too big, but the model is less sensitive to α. Based on these results, our last experiment, ABRJI, was run with a drastically reduced K_{min} (see Table 1) to see if we can reduce the errors further. As we have seen in the above, the result shows a significant improvement in error reduction. The biharmonic constant GM diffusion was necessary to suppress grid scale noise when K_{min} is small.

5 Discussion and Conclusion

To understand how we are able to change the model errors by changing the GM parameterization, we can directly measure the GM transports and their contributions to the model tendencies for tracers. We choose to compare two typical experiments in the North Atlantic sector. Figure 7 compares the zonal mean eddy induced transports ($\overline{v^*}$) in the North Atlantic for ABRJC and ABRJD. Potential density contours are also superimposed to help us understand how GM works. The dark areas shows the northward transport and the light areas southward. From the top panel of Fig.7 (ABRJC), one can clearly see that the eddy induced transports form two extra overturning cells in the subtropical and subpolar gyres in the upper ocean. Strong northward transport occurs near $45°N$ and $65°N$ around 200m depth. The southward transport near $65°N$ in the deeper ocean showing the bottom dense water overflows from the straits. Comparing Fig.7 with figures 5 and 6, particularly Fig.6, it is not difficult to understand how the GM scheme may contribute to the salinity errors in ABRJC and the HadCM3 control run (AAYFA as the early part). By reducing the GM coefficient, we have reduced the eddy induced overturning (see the bottom panel of Fig.7).

How the change of the GM scheme contributes to the reduction of model errors can also be revealed by the GM contribution to the total rate of change diagnostics from the tracer equations. All the individual items in the tracer equations are diagnosed when the model was integrated forward. Corresponding to Fig.7, Fig.8 shows the average GM contributions to the total rate of change in the North Atlantic for experiments ABRJC and ABRJD. Generally in the global zonal mean (figures not given), GM makes significant contributions to the tendency in three major regions: the upper 200m of the southern ocean and the northern mid-latitudes, which are associated with the Antarctic circumpolar current (ACC) and the Gulf Stream, and the whole column down to 1000m depth around $65°N$ which is associated with the North Atlantic deep convection and bottom outflows. The GM scheme is designed to mainly parameterize eddies in the thermocline, but it also has a big impact in the regions of bottom dense water outflows such as the North Atlantic (Hirst and McDougall, 1996) and the eastern Mediterranean (Haines and Wu, 1998), where deep water formation occurs in marginal seas and then flows out of straits. In these areas, because of the existence of strong density or potential vorticity gradients the GM scheme helps the overflows and reduces the undesirable overmixing in z-coordinate models without specific boundary layer schemes. This is reflected in the large vertical extents of strong GM contributions around $65°N$ seen in Fig.7 and Fig.8. Comparing the left (ABRJC) to the right (ABRJD), the reduction of K_{min} in ABRJD has very effectively removed those GM contributions to the total rate of change at intermediate depth in the subtropics and northern mid-latitudes, which are largely responsible for the model errors shown in Fig.5 and Fig.6. The change of α is mainly reflected in the Southern Ocean, which can be seen by comparing ABRJD and ABRJF (figures not shown). A larger value of α (0.045 compared to 0.0075) has an increased GM contribution to the total rate of change seen in the southern ocean.

The comparison of the 4 experiments has indicated that the GM scheme is at least partially responsible for the model errors of sub-surface water mass properties seen in the HadCM3 control run. This can be seen from the pattern correlation of the model errors and the GM contributions to the total rate of change in the tracer tendency diagnostics. More important is that these errors can be changed by modifications to the GM parameters, particularly the minimum eddy mixing coefficient K_{min} applied to large parts of the oceans. Experiment ABRJI shows the best reduction of model errors compared to others. This has been achieved by a reduction of K_{min} from $350m^2s^{-1}$ to a minimal value of $10m^2s^{-1}$ with the help of a constant biharmonic GM diffusion.

The model seems to be more sensitive to the change of K_{min} than to α. This because K_{min} affects large parts of the oceans while α mainly affects the regions associated with the western boundary currents and ACC. The question is what value of eddy mixing coefficient should we use in the large parts of oceans where the large-scale isopycnal slopes are small or baroclinic instabilities are weak? In theory, given the efficiency coefficient α, the GM coefficient K should be evaluated according to the large-scale density structures. However, a minimum value is required to keep the numerical noise down. The choice we made for experiment ABRJI seems to produce a good compromise. The optimal parameters would require further fine tuning.

The so-called "model errors" may have resulted from many contributing factors, particularly processes acting at the air-sea interface and within the ocean mixed layer. The GM scheme only helps to redistribute water properties in the interior ocean. By tuning the eddy parameterization scheme, the errors can be reduced but we may not be able to eliminate them completely.

References

Bryan, K., J.K. Dukowicz and R.D Smith, 1999: On the mixing coefficient in the parameterision of bolus velocity. *J. Phys. Oceanogr.*, **29**, 2442-2456.

Danabasoglu, G., and J.C McWilliams, 1995: Sensitivity of the global ocean circulation to parameterisations of mesoscale tracer transports. *J. Climate*, **8**, 2967-2987.

Gent, P.R. and J.C. McWilliams, 1990: Isopycnal mixing in ocean circulation models. *J. Phys. Oceanogr.*, **20**, 150-155.

Gent, P.R., J. Willebrad, T.J. McDougall, and J.C. McWilliams, 1995: Parameterising eddy-induced tracer transports in ocean circulation models. *J. Phys. Oceanogr.*, **25**, 463-474.

Gordon, C., C. Cooper, C.A. Senior, H. Banks, J.M. Gregory, T.C. Johns, J.F.B. Mitchell and R.A. Wood, 1999: The simulation of SST, sea ice extents and ocean heat transports in a version of the Hadley Centre coupled model without flux adjustments. Submitted to *Climate Dynamics*.

Green, J.S, 1970: Transfer properties of the large-scale eddies and the general circulation of the atmosphere. *Quart. J. Roy. Met. Soc.*, **96**, 157-185.

Haines, K. and P. Wu, 1998: GCM studies of intermediate and deep waters in the Mediterranean. *J. Marine Systems*, **18**, 197-214.

Held, I.M. and V.D. Larichev, 1996: A scaling theory for horizontally homogeneous, baroclinically unstable flow on a beta plane. *J. Atmos. Sci.*, **53**, 946-952.

Hirst, A.C, and T.J. McDougall, 1996: Deep-water properties and surface buoyancy flux as simulated by a z-coordinate model including eddy-induced advection. *J. Phys. Oceanogr.*, **26**, 1320-1343.

Klinker, E. and P.D. Sardeshmukh, 1992: The diagnosis of mechanical dissipation in the atmosphere from large-scale balance requirements. *J. Atmos. Sci.*, **49**, 608-627.

Milton, S.F., 1994: Diagnosing the source of systematic errors in the U.K. Meteorological Office global unified model. WMO/TD-No.592, pp.6.11-6.13.

Roberts, M., and D. Marshall, 1998: Do we require adiabatic dissipation schemes in eddy-resolving ocean models? *J. Phys. Oceanogr.*, **28**, 2050-2063.

Spall, M.A., and D.C. Chapman, 1998: On the efficiency of baroclinic eddy heat transport across narrow fronts. *J. Phys. Oceanogr.*, **28**, 2275-2287.

Stone, P.H., 1972: A simplified radiative-dynamical model for the static stability of rotating atmosphere. *J. Atmos. Sci.*, **29**, 405-418.

Treguier, A.M., I.M. Held, and V.D. Larichev, 1997: On the parameterisation of quasi-geostrophic eddies in primitive equation ocean models. *J. Phys. Oceanogr.*, **27**, 567-580.

Visbeck, M., J. Marshall, T. Haine, and M. Spall, 1997: On the specification of eddy transfer coefficients in coarse resolution ocean circulation models. *J. Phys. Oceanogr.*, **27**, 381-402.

Wright, D.K., 1997: A new eddy mixing parameterisation in a ocean general circulation model. *WOCE Newsletter*, **26**, 27-29.

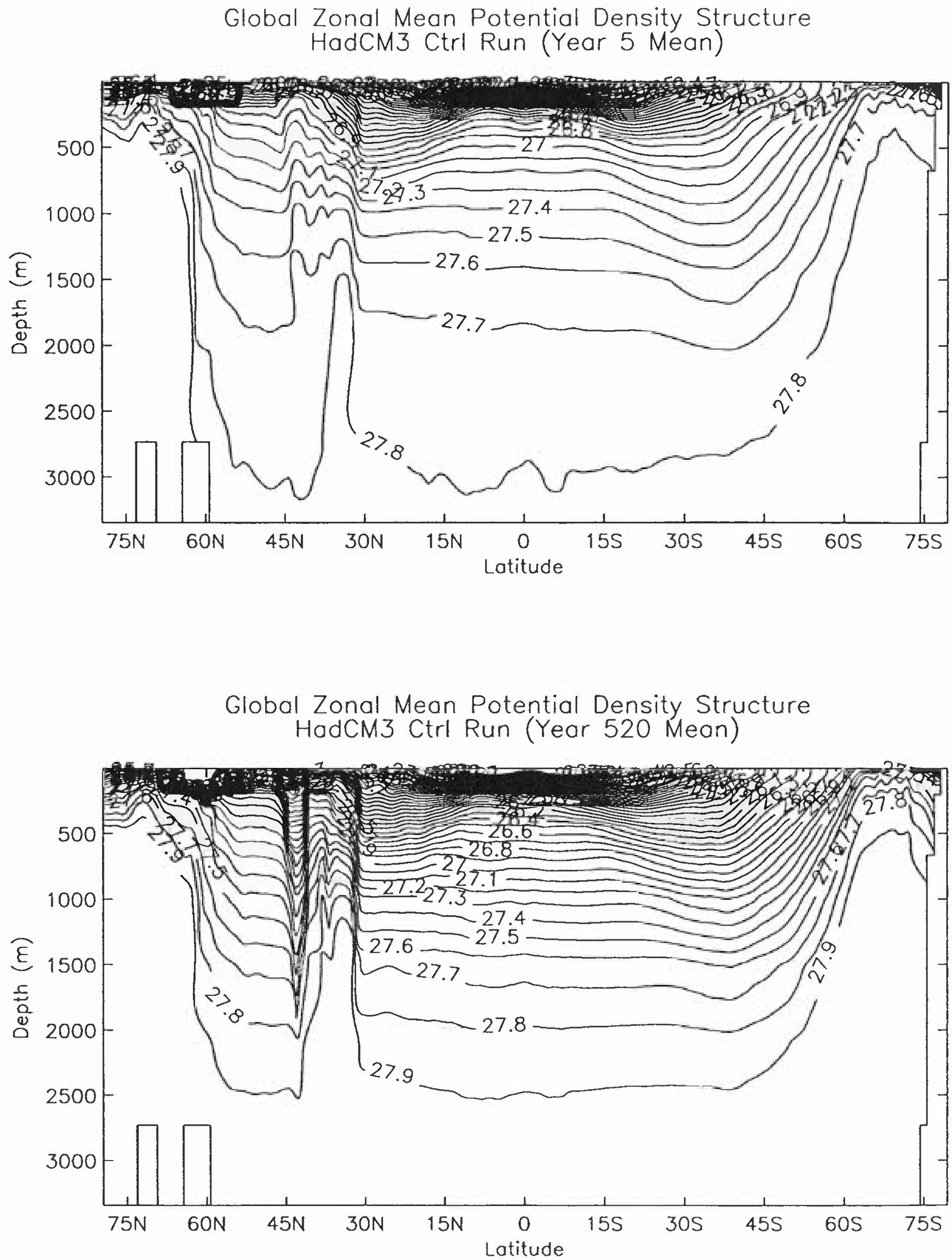

FIG.1 *Global zonal mean potential density structures for year 5 (top) and year 520 (bottom) of the HadCM3 control run, showing an increase of density in the deep oceans.*

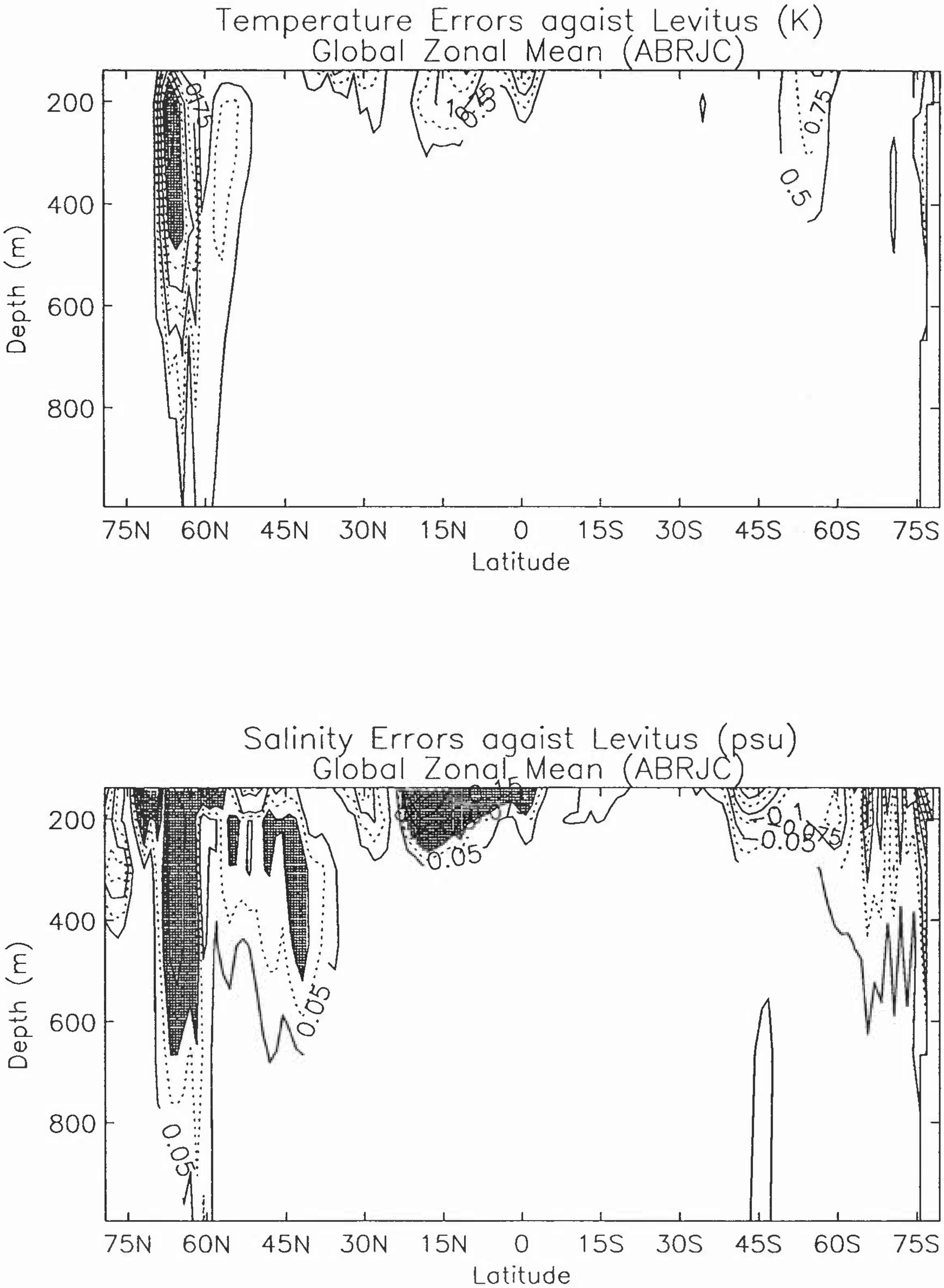

FIG.2 *Global zonal mean temperature and salinity errors (model against Levitus) for the control run averaged over the 10 years of model integration. Contour interval for temperature is 0.25°C and the shaded areas are where temperature errors exceed 2°C. Contour interval for salinity is 0.025psu and shaded are where salinity errors are greater than 0.1psu.*

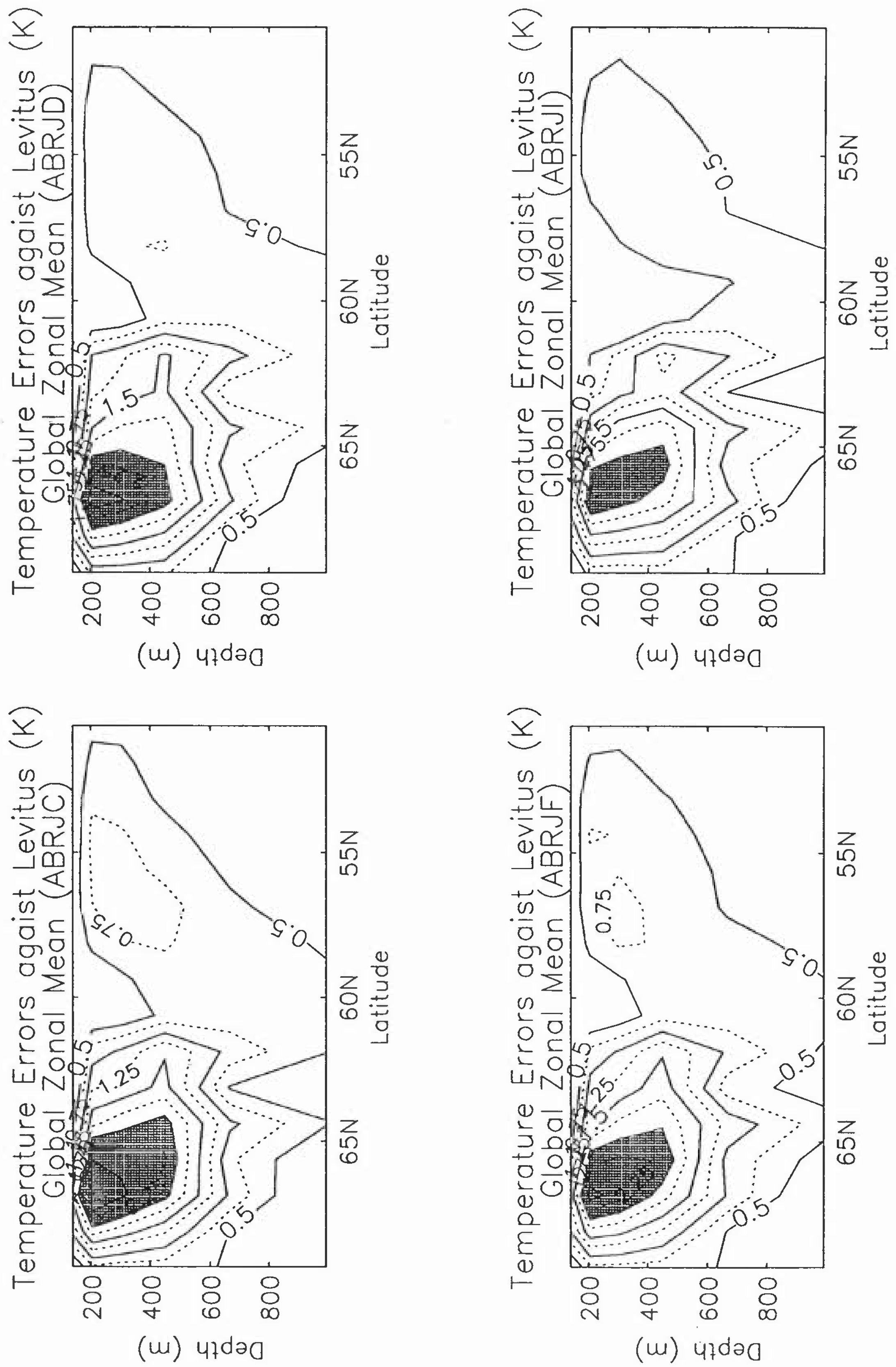

Fig.3 *Comparison of global zonal mean temperature errors averaged over the 10 years of model integration for the 4 experiments. Contour interval is* $0.25°C$ *and shaded are areas where temperature errors are greater than* $2°C$.

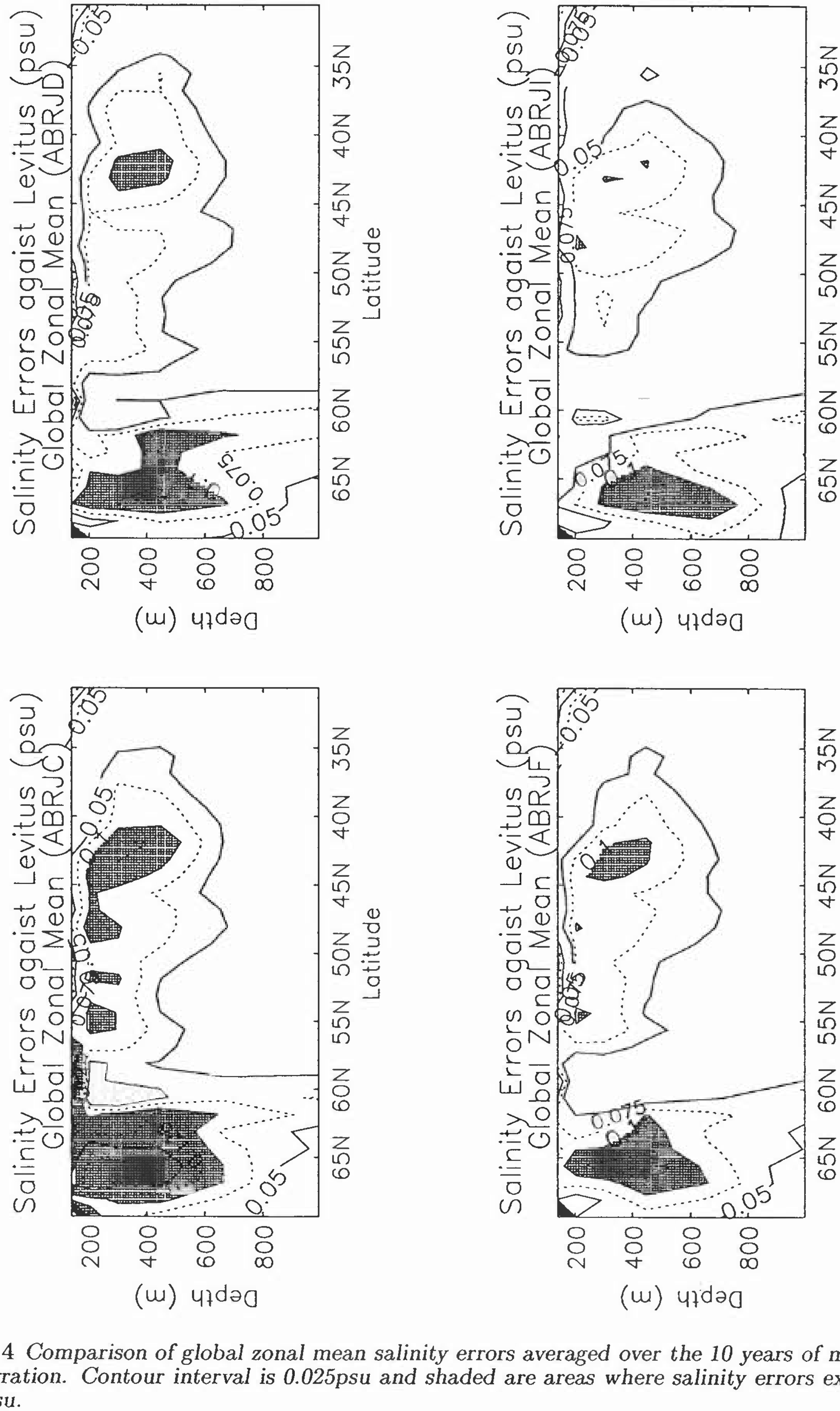

FIG.4 *Comparison of global zonal mean salinity errors averaged over the 10 years of model integration. Contour interval is 0.025psu and shaded are areas where salinity errors exceed 0.1psu.*

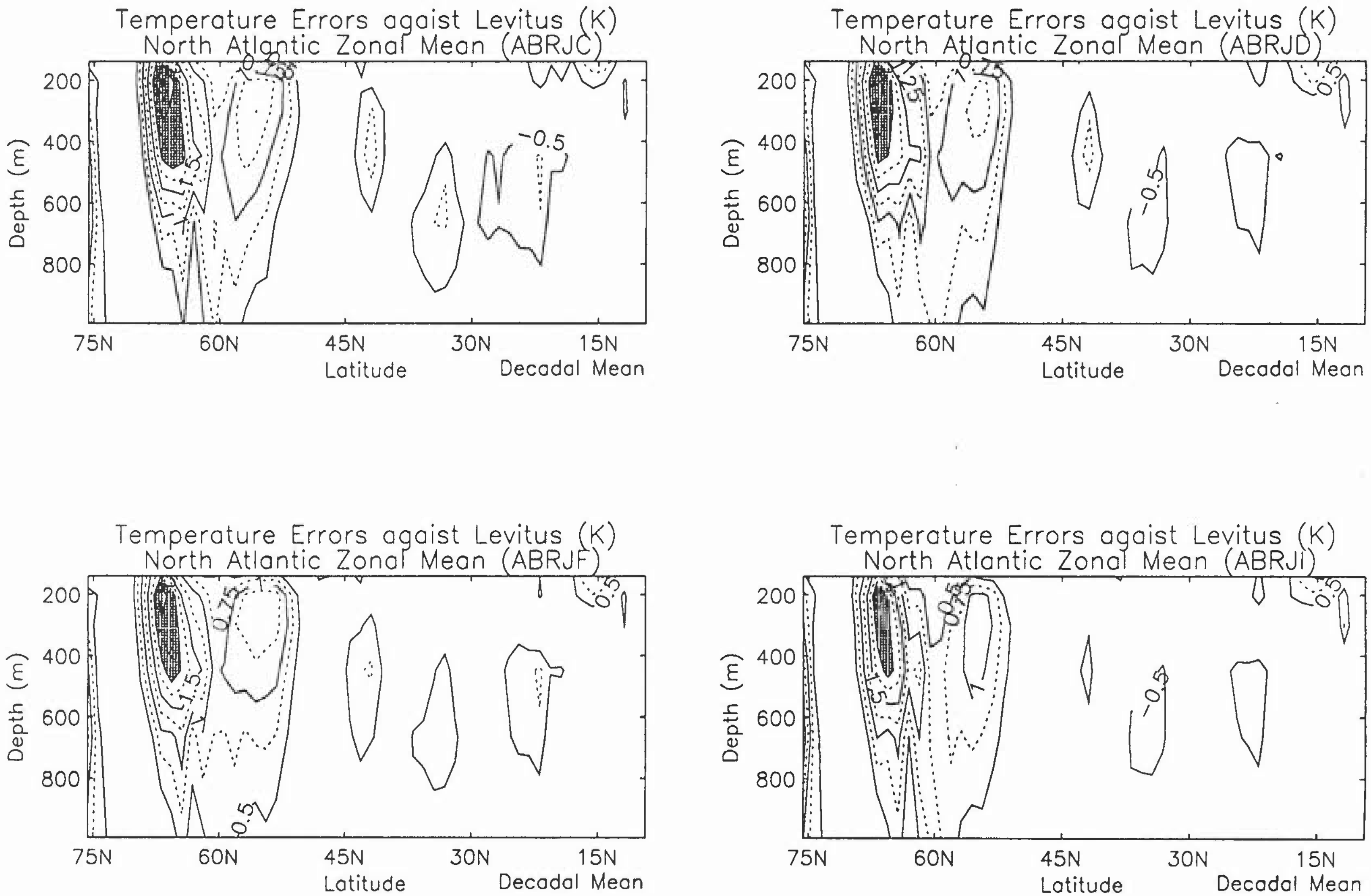

FIG.5 *North Atlantic zonal mean temperature errors averaged over the 10 years of model integration. Contour interval is 0.25°C and shaded are areas where temperature errors are greater than 2°C.*

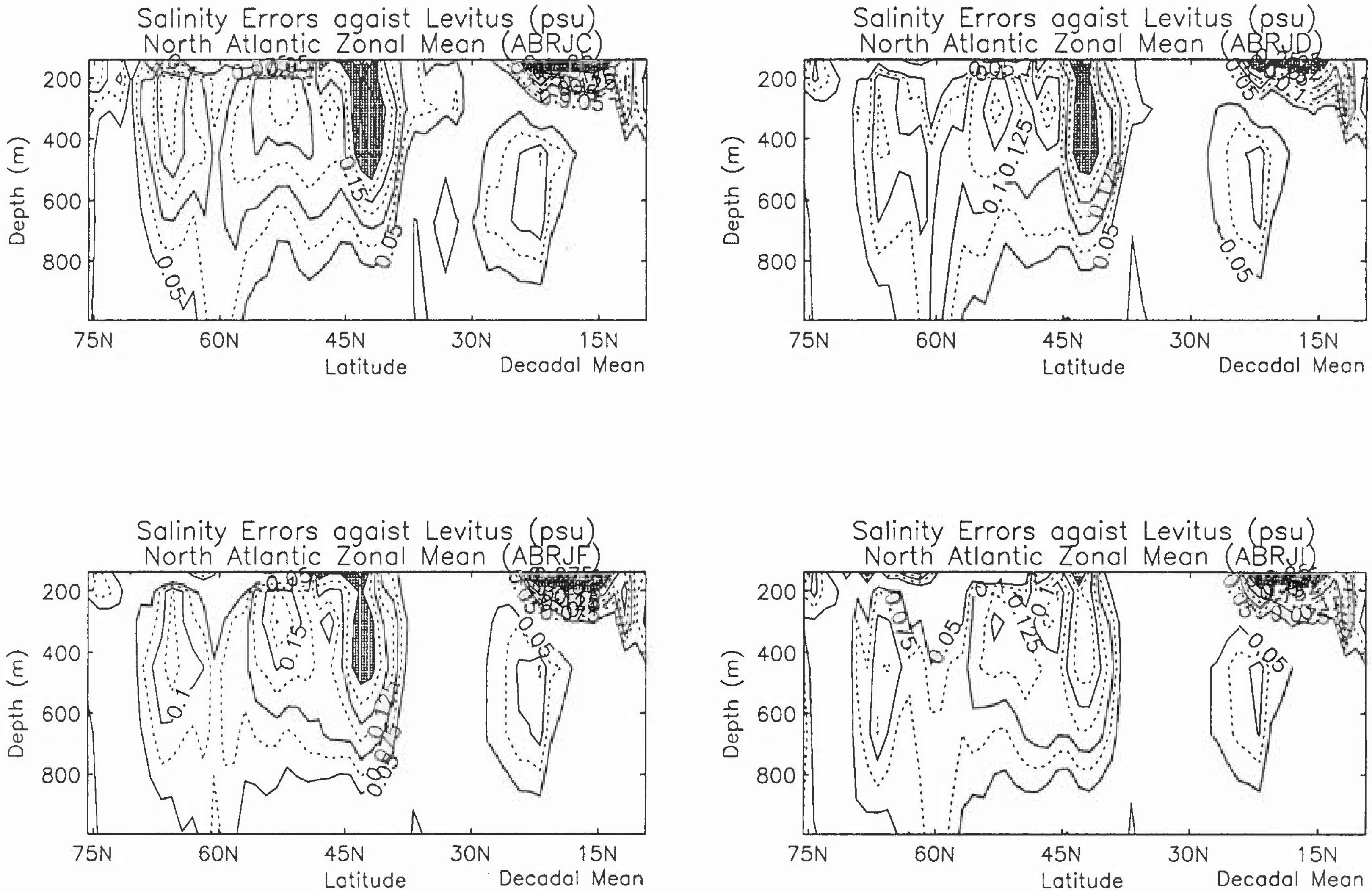

FIG.6 *North Atlantic zonal mean salinity errors averaged over the 10 years of model integration. Contour interval is 0.025psu and shaded are areas where salinity errors exceed 0.1psu.*

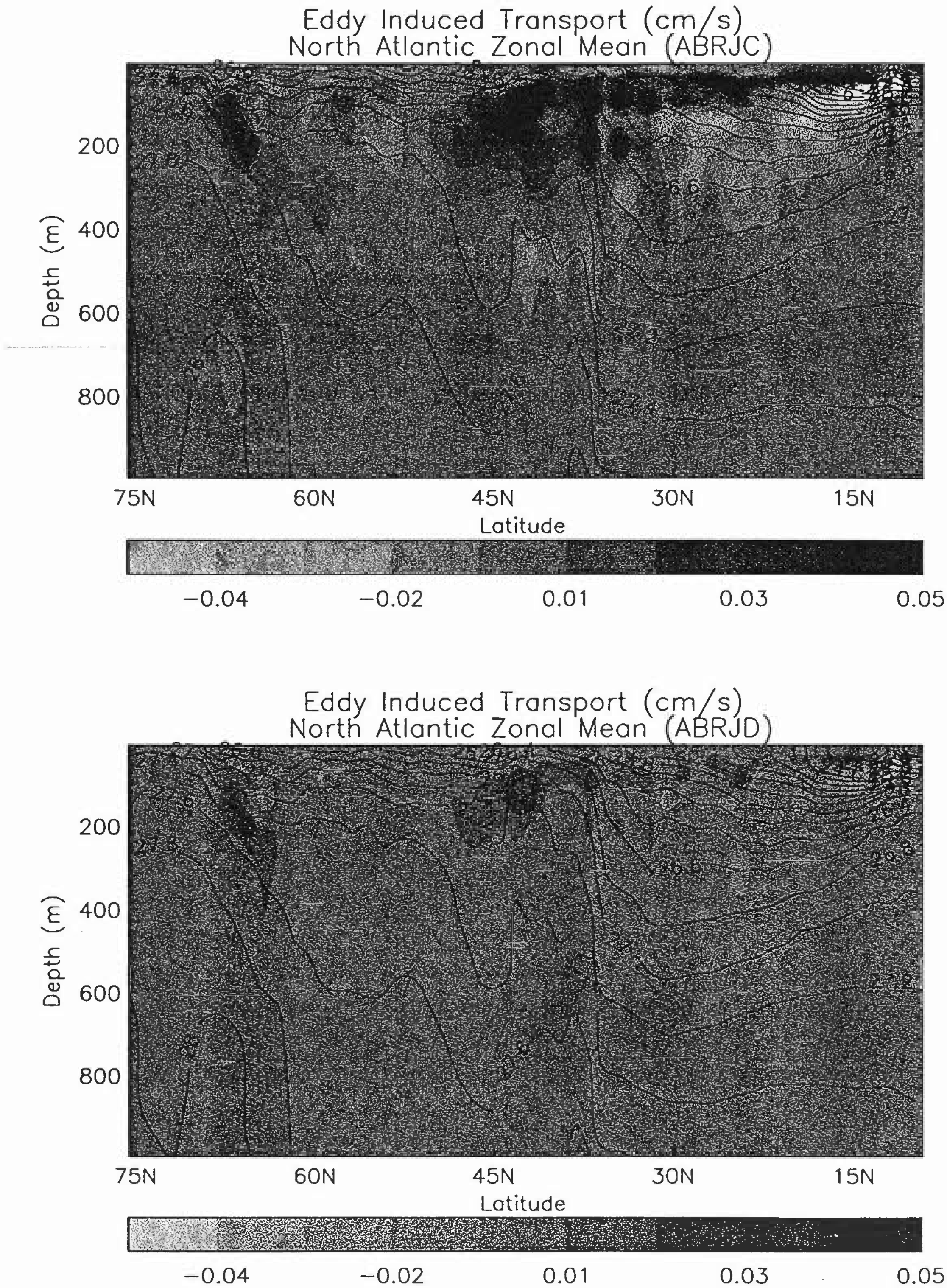

FIG.7 *North Atlantic zonal mean density structure and eddy induced transport for comparison between experiments ABRJC and ABRJD to show how GM parameterisation contribute to the meridional transports and the effect of reduced GM coefficient. Contours are potential density and the background shading shows the eddy induced transport. Dark colours indicate northward transport and light southward.*

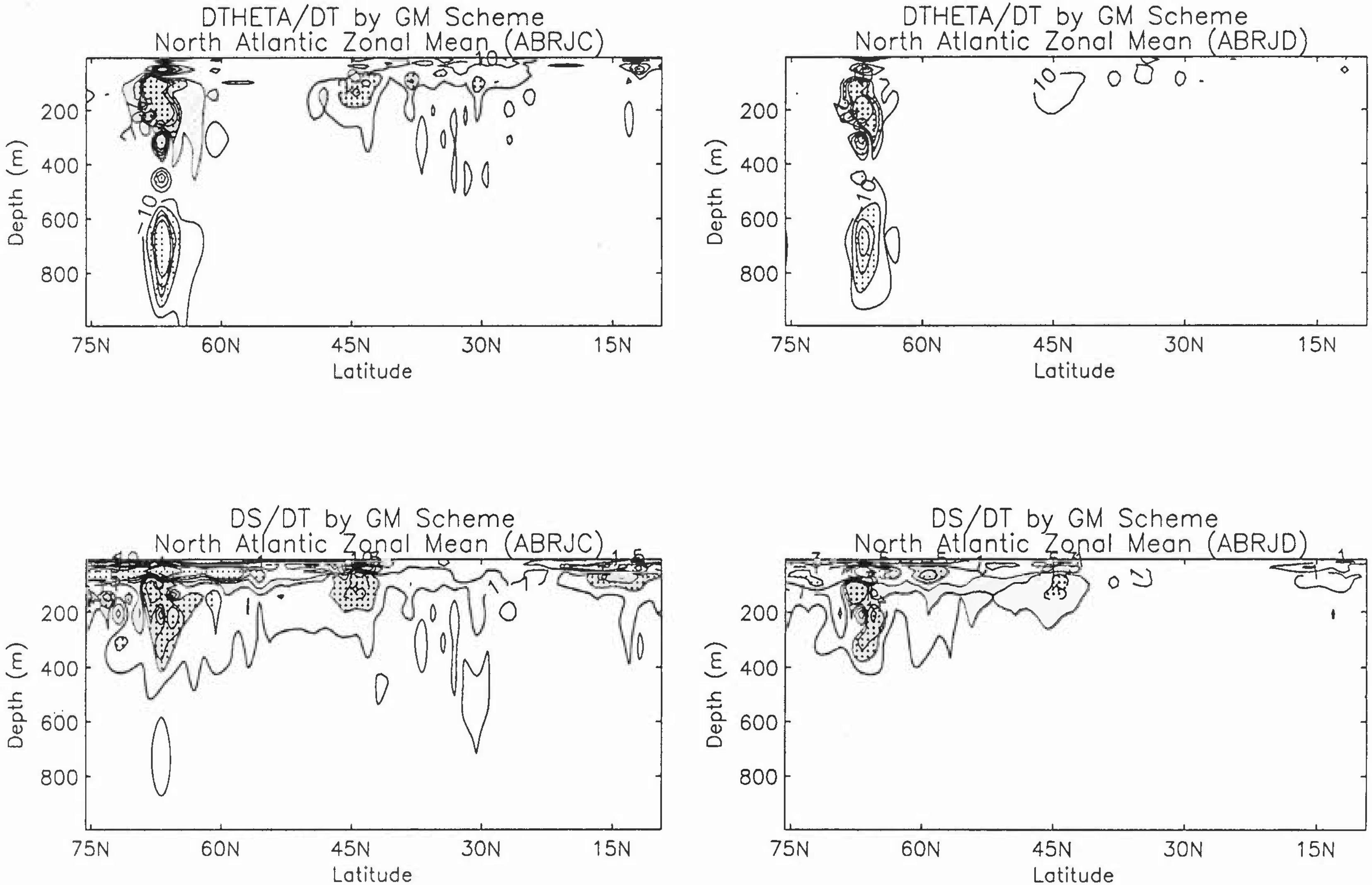

FIG.8 North Atlantic zonal mean GM contributions to the total rates of change for temperature and salinity averaged over the 10 years of model integration.